

## Chapter 17

# Analysis of the Combined Effects of Resveratrol and Radiation on Lung Cancer Cells

Carolina S Moreno<sup>1,3</sup>, Sizie O Rogero<sup>1\*</sup>, Andrés J Galisteo Jr.<sup>2</sup>, Daniel P Vieira<sup>1</sup>, Áurea S Cruz<sup>4</sup>, Roberto K Sakuraba<sup>3</sup>, Eduardo Weltman<sup>3</sup> and José R Rogero<sup>1</sup>

<sup>1</sup>Instituto de Pesquisas Energéticas e Nucleares – IPEN - CNEN/SP - Av. Lineu Prestes, Brazil

<sup>2</sup>Instituto de Medicina Tropical de São Paulo – USP - Av. Dr. Enéas de Carvalho Aguiar, Brazil

<sup>3</sup>Hospital Israelita Albert Einstein - Av. Albert Einstein, Brazil

<sup>4</sup>Instituto Adolfo Lutz - Av. Dr Arnaldo, Brazil

**\*Corresponding Author:** Sizie O Rogero, Instituto de Pesquisas Energéticas e Nucleares – IPEN - CNEN/SP - Av. Lineu Prestes, 2242 – 05508-900 - São Paulo, SP, Brazil, Email: sorogero@ipen.br

First Published **June 11, 2018**

This Book Chapter is an excerpt from an article published by Sizie O Rogero, et al. at Integrative Cancer Biology & Research in May 2017. (Moreno CS, Rogero SO, Galisteo Jr. AJ, et al. Analysis of the Combined Effects of Resveratrol and Radiation on Lung Cancer Cells. Integr Canc Biol Res 2017; 1:005.)

**Conflict of Interest:** The authors declare that there are no conflicts of interest.

Copyright: © 2018 Sizue O Rogero, et al.

*This article is distributed under the terms of the Creative Commons Attribution 4.0 International License (<http://creativecommons.org/licenses/by/4.0/>), which permits unrestricted use, distribution, and reproduction in any medium, provided you give appropriate credit to the original author(s) and the source.*

## Abstract

Mucoepidermoid lung carcinoma is frequently manifested by obstructive trachea symptoms. It is necessary to develop effective curative or palliative therapeutic strategies for treating mucoepidermoid lung carcinoma through administration of compounds that improve ionizing radiation treatment, thereby increasing the effects of the treatment on tumor cells while minimizing the effects on normal tissues surrounding the tumor cells. Resveratrol is a polyphenolic phytoalexin present in wines and several plants and has a broad spectrum of biological activities, including antioxidant and anticarcinogenic effects. The biological effects of ionizing radiation plus resveratrol have been examined in different types of cell in many studies. Here, we aimed to verify the effects of resveratrol on mucoepidermoid lung carcinoma cells NCI-H292 exposed to ionizing radiation. *In vitro* studies in NCI-H292 cell culture using neutral red uptake assays showed that the cytotoxicity index ( $IC_{50}$ ) of resveratrol was 401.5  $\mu$ M, and the lethal dose 50 % ( $LD_{50}$ ) of ionizing radiation in the absence of resveratrol was 693 Gy. *In vitro* micronucleus assays were then performed to verify the genotoxic effects of resveratrol, and fluorescence assays were performed to evaluate the effects of resveratrol on the cell cycle, repair and injury processes, cellular necrosis, and apoptosis. The results demonstrated that 30  $\mu$ M resveratrol promote injury on NCI-H292 cells after 24 h of irradiation. Therefore, this study provides results able to support *in vitro* future investigations about radiosensitive potential of resveratrol in lung cancer cells. There is a need to investigate compounds with potential to improve the local control of

lung cancer promoted by radiation therapy. This way avoiding injuries to healthy cells.

## Keywords

Resveratrol; Ionizing Radiation; Lung Cancer Cells; Micronucleus Assays; Fluorescence Assays; Cytotoxicity Assay

## Abbreviations

ANOVA-Analysis of Variance; BNCs-Binucleated Cells; CBPI-Cytokinesis Block Proliferation Index; CT-Computed Tomography; DVHs-Dose-Volume Histograms; EDTA-Ethylendiaminetetraacetic Acid Solution; ELISA-Automated Enzyme-Linked Immunosorbent Assay; FAPESP-Fundação de Amparo à Pesquisa do Estado de São Paulo; FBS-Fetal Bovine Serum; IC<sub>50</sub>-Cytotoxicity Index; IMRT-Intensity Modulated Radiation Therapy; LD<sub>50</sub>-Lethal Dose 50 %; MN-Micronucleus; M phase: Mitosis Phase; NCI-H292 Cells-Mucoepidermoid Lung Carcinoma Cells; NCTC L929 Cells-Mouse Fibroblast Cell Line; NCI-H838 Cells-Human Non-Small Cell Lung Cancer; OD-Optical Density; PBS-Phosphate Buffered Saline; PI-Propidium Iodide; RPMI-Use-RPMI-1640 Medium Containing 10 % Fetal Bovine Serum; SEMs-Standard Errors of the Means; S phase-Synthesis phase

## Introduction

Lung cancer is associated with high mortality rates and has been shown to have an increasing incidence worldwide [1]. One type of lung cancer, mucoepidermoid lung carcinoma, arises from minor salivary gland tissue of the proximal tracheobronchial tree. It is frequently manifested by irritation and obstructive symptoms and tends to spread locally, compromising the trachea [2-4].

Radiation therapy is an effective curative or palliative treatment for many types of cancer. Its benefits are associated with gaining local or regional control over the tumor by exposure to clinically tolerated doses of ionizing radiation. Chemotherapy is another effective mo-

dality of cancer treatment that aims to decrease the number of tumor cells and prevent distant metastases. Chemotherapy also improves the effects of ionizing radiation on local tumor control. Therefore, radiation therapy associated with chemotherapy tends to result in major improvements in survival rates for patients with cancer [5,6].

Resveratrol (3,4',5-trihydroxy-trans-stilbene) is a natural phenolic phytoalexin that is abundant in grapes, wine, peanuts, and a variety of other plant-based food sources.

Resveratrol is produced by several plants in response to injury caused by bacterial or fungal infections, exposure to ultraviolet light, or exposure to chemical agents. These conditions may occur individually or in combination [7]. Growing evidence suggests that resveratrol exerts radioprotective effects, acting as a scavenger of free radicals produced during several biological processes [8]. These effects make resveratrol an important potential therapeutic agent in a variety of pathological processes, such as cancer [9]. Resveratrol has also been shown to exert radiosensitizing effects in certain types of tumor cells, blocking cell cycle progression and inducing apoptotic and necrotic cell death [10,11]. Resveratrol has been reported to have activity against lung cancer; recent studies have shown that resveratrol increases the cytotoxic effects of radiation on lung cancer cells by significantly enhancing radiation-induced cell death [12,13].

In this study, we aimed to evaluate the biological effects of resveratrol in NCI-H292 cells culture exposed to ionizing radiation.

We assessed the radiation dose that induces the death of 50 % ( $LD_{50}$ ) of cell population and the resveratrol cytotoxicity studies ( $IC_{50}$ ), as well as the genotoxic effects of resveratrol. Additionally, we examined the effects of resveratrol on cell cycle synchronization, DNA repair, and cell injury/cell death processes. The results of this study demonstrated the importance of further *in vitro* investigations about the radiosensitizing potential of resveratrol on lung cancer cells.

## Materials and Methods

### Reagents and Equipment

Resveratrol was purchased from FarmaNostra (Anápolis, GO, Brazil). The other reagents were PA grade and from Sigma-Aldrich (São Paulo, SP, Brazil) and Merck (São Paulo, SP, Brazil). The human lung mucoepidermoid carcinoma cell line NCI-H292 was obtained from American Type Culture Collection (ATCC CRL-1848; Manassas, VA, USA).

To obtain greater precision, accuracy, and conformability of ionizing radiation dose distributions in the cells culture, a computed tomography (CT) scanner (LightSpeed RT16; General Electric; Buckinghamshire, United Kingdom), and a treatment planning system (Eclipse, version 11; Varian Medical System, Inc.; Palo Alto, CA, USA) were used. Radiation doses were delivered as a single fractional dose via the TrueBeam Radiotherapy System (Varian Medical Systems), in the presence of 0, 15, 30, and 60  $\mu\text{M}$  resveratrol concentrations. These procedures were performed at Hospital Israelita Albert Einstein, São Paulo, Brazil.

### CT Scanning and Treatment Planning Process

CT scans were performed using 24-well microplates. Slabs of Solid Water Phantom (4.0 cm thick; Gammex RMI, Wisconsin, USA) and tissue-equivalent material (bolus material, 1.0 cm thickness; CIVCO Medical Solutions, Iowa, EUA) were placed directly above and below the microplate surface to avoid the surface sparing effect in the megavoltage photon beam. CT images were acquired using a Light-Speed RT16 systems with the following parameters: 140 kV, 180 mA, 1.25 mm slice thickness, and  $512 \times 512$  matrix.

Irradiation plans were created with Eclipse Treatment Planning System software using the Analytical Algorithm Anisotropic dose calculation algorithm (AAA, version 13, Varian Medical System). CT images were directly displayed on the Eclipse Treatment Planning System. Volumes of structures of interest were hand-contoured, slice

by slice. The microplate arrangement was outlined to obtain volumetric image data, and each well of microplate was defined as a target volume.

Irradiation procedures were planned for a single fraction of different doses (0.8, 5, and 10 Gy), using a photon energy of 6 MV and a dose rate of 14 Gy/min from the TrueBeam radiotherapy system. Intensity Modulated Radiation Therapy (IMRT) plans were performed using multileaf collimator (MLC) with posterior fields. Dose calculations and plan evaluations were performed by analyzing dose distributions in CT images, dose statistics, and dose-volume histograms (DVHs).

## Cell Culture

NCI-H292 cells were cultured in RPMI-1640 medium containing 10 % fetal bovine serum (FBS), without antibiotics, designated as “RPMI-use”. Culture was incubated at 37° C in a 5 % CO<sub>2</sub> humidified atmosphere until cell monolayer formation occurred. Culture was then treated with 0.20 % trypsin and 0.02 % ethylenediaminetetraacetic acid (EDTA) solution. The cell suspension was adjusted for each assay after counting in a Neubauer chamber.

## Cytotoxicity Assay

The cytotoxicities of resveratrol, colchicine and hydroxyurea were assessed by neutral red uptake assays, as previously described [14,15].

Ninety-six-wells microplates containing  $9.0 \times 10^4$  cells in each well were cultured overnight in a CO<sub>2</sub> humidified incubator at 37° C. NCI-H292 cells were then exposed to 0.2 mL of resveratrol, colchicine, or hydroxyurea solution, serially diluted with RPMI-use. Resveratrol solution was used at concentrations of 100 %, 50 %, 25 %, 12.5 %, and 6.25 %, corresponding to 500, 250, 125, 62.5, and 31.25 µM. Colchicine was used at concentrations of 128, 64, 32, 16, and 8 µg/mL. Hydroxyurea was used at concentrations of 25.6, 12.8, 6.4, 3.2, and 1.6 mg/mL. The positive-control (latex extract) and negative-control

(HDPE extract) solutions were used at 100 %, 50 %, 25 %, 12.5 %, and 6.25 % extract dilution. Next, 0.2 mL of diluted controls, resveratrol, colchicine, and hydroxyurea solutions were added to respectively well, and 0.2 mL fresh RPMI-use was added to the control wells.

All samples were tested in triplicate. The microplate was incubated for 24 h at 37° C in a 5 % CO<sub>2</sub> humidified incubator. After incubation, the culture medium was replaced by culture medium containing neutral red, and the microplate was incubated again for 3 h at 37° C. The dye-containing medium was then discarded, and the microplate was washed twice with phosphate buffered saline solution (PBS) and once with 1 % calcium chloride in 0.5 % formaldehyde solution. Next, 0.2 mL extraction solution (50 % ethanol in 1% acetic acid) was added to each well to promote cell rupture and neutral red release. Dye absorbance was measured at 540 nm using an automated enzyme-linked immunosorbent assay (ELISA) plate reader (Sunrise; Tecan Group Ltd., Männedorf, Switzerland). Cell survival percentages were determined in relation to control cell optical density (OD), considered 100 % of cell viability.

## Lethal Dose of Ionizing Radiation

To determine the LD<sub>50</sub>, 96-well microplates containing  $9.0 \times 10^4$  NCI-H292 cells in each well were kept overnight in a CO<sub>2</sub> humidified incubator at 37° C. Prior to irradiation of the microplates containing cells, the culture medium was replaced with PBS (pH 7.4).

Radiation doses were delivered using a TrueBeam radiotherapy system at 14 Gy/min dose rate, 6 MV energy, with different doses (250, 500, 750, and 1,000 Gy) in a single fraction at room temperature (19 – 21° C). Nonirradiated cells, used as control, were kept in darkness at room temperature during the irradiation of the other microplates.

After irradiation, the PBS in each microplate well was replaced by RPMI-use, and the microplates were then incubated at 37° C in a 5 % CO<sub>2</sub> humidified atmosphere for 24 h. Subsequent procedures for neutral red dye incorporation, microplates washing, OD reading, and

the cell viability percentage were performed as described above for the cytotoxicity assays (item 2.4).

## Preparation of Resveratrol, Colchicine, and Hydroxyurea Solutions

For micronucleus assays and fluorescence tests, a resveratrol stock solution was prepared at 25 mM in ethanol. From this solution, three different dilutions were made in RPMI-use, yielding 15, 30 and 60  $\mu\text{M}$  resveratrol concentrations. Colchicine and hydroxyurea were used as references for mitosis phase and synthesis phase arrest of cell cycle progression; used solutions were 0.08  $\mu\text{g}/\text{mL}$  for colchicine and 152.12  $\mu\text{g}/\text{mL}$  for hydroxyurea dissolved in RPMI-use. All solutions were sterilized by passing through a 0.22  $\mu\text{m}$  pore membrane system.

## Micronucleus (MN) Assays

MN assays was performed in triplicate. 500  $\mu\text{L}$  of cell suspension containing  $1.0 \times 10^5$  cells/mL was placed on a coverslip within a Petri dish. After cells adhesion onto the coverslip, 1.5 mL RPMI 1640 medium was added, and the Petri dish was kept in a  $\text{CO}_2$  humidified incubator for 48 h. The culture medium was replaced with 5 mL resveratrol solution. Dishes were then incubated for 24 h at 37° C in a 5 %  $\text{CO}_2$  humidified atmosphere. Prior to irradiation, the resveratrol solution was replaced by PBS (pH 7.4).

Irradiation of cells culture was performed using a TrueBeam radiotherapy system at different doses of 0.8, 5, and 10 Gy, at dose rate of 14 Gy/min in a single fraction at room temperature. Nonirradiated cells, used as control, were kept in darkness at room temperature while the other samples were irradiated. After irradiation, the PBS in each dish was replaced with RPMI 1640 medium containing cytochalasin B (4  $\mu\text{g}/\text{mL}$ ). The dishes were then incubated for 48 h at 37° C in a 5 %  $\text{CO}_2$  humidified atmosphere.

The coverslips containing cells were washed once with PBS, treated with isotonic saline solution (0.9 % NaCl) for 15 min, fixed

with 4 % formaldehyde in water for 15 min, and washed three times with PBS. Fixed cells on coverslip were stained with acridine orange (0.003 % in PBS) and deposited onto histological slide (26 × 76 mm) for microscopic analysis.

Visualization of MNs was performed using a fluorescence microscope with appropriate filters following pre-established protocols for cells with blocked cytokinesis [16-18]. For our analyses, it was counted only binucleated cells with intact cytoplasm and a minimum of 1,000 cells per concentration of resveratrol; mononuclear cells (one nucleus per cell) and multinucleated cells (three or more nuclei per cell) were also counted for statistical calculations.

### Cell Cycle, DNA Repair, and Cell Injury Analyses by Fluorescence

Twenty-four-wells microplates containing  $1.7 \times 10^5$  cells in each well were kept overnight in a CO<sub>2</sub> humidified incubator at 37° C. NCI-H292 cells were then exposed to resveratrol, colchicine, or hydroxyurea solutions for 24 h. Whereas control cells were incubated with single RPMI-use. Resveratrol, colchicine, and hydroxyurea exposure experiments were carried out in four replicates. Prior to microplates irradiation, the solutions were replaced with PBS (pH 7.4).

Microplates irradiation was performed using a TrueBeam radiotherapy system. Cells were exposed to 0.8, 5 or 10 Gy at a dose rate of 14 Gy/min in a single fraction at room temperature. Nonirradiated cells were used as control cell and were kept in the darkness at room temperature during the other samples irradiation.

The cells were analyzed 3 and 24 h after irradiation. For analyses of 3 h after irradiation, the cells were stained with ethidium bromide solution (0.2 µg/mL) for 5 min at room temperature in the dark. The ethidium bromide solution was then replaced by PBS, and fluorescence intensity was measured using a FilterMax F5 Multi-Mode Microplate Reader (Molecular Devices, Sunnyvale, CA, USA). For analy-

ses at 24 h after cell irradiation, the PBS was replaced with RPMI-use immediately after irradiation, and the microplates were incubated for 24 h at 37°C in a 5% CO<sub>2</sub> humidified atmosphere. Before the examination, the cells were stained with ethidium bromide (0.2 µg/mL) for 5 min at room temperature in the dark, and fluorescence intensity was measured.

## Fluorescence Analysis of Apoptotic and Necrotic Cells

Twenty-four-wells microplates containing  $1.7 \times 10^5$  cells in each well were kept overnight in a CO<sub>2</sub> humidified incubator at 37°C. Cells were then exposed to resveratrol, colchicine, or hydroxyurea for 24 h. Control cells received only RPMI-use. Resveratrol, colchicine, and hydroxyurea exposure experiments were carried out in four replicates. Prior to microplates irradiation, solutions were replaced with PBS (pH 7.4). Microplates irradiation was performed using a TrueBeam radiotherapy system. Cells were exposed to 0.8, 5, or 10 Gy doses and 14 Gy/min dose rate in a single fraction at room temperature. Nonirradiated cells were used as control and were kept in darkness at room temperature during the irradiation of the other samples.

Apoptotic and necrotic cells were then identified using an annexin V-FITC apoptosis detection kit (Sigma-Aldrich Chemical Co, St. Louis, MO) according to the manufacturer's instructions. After 24 h of irradiation, the cells were treated with staining solution containing annexin V-FITC and propidium iodide (PI). After 10 min of incubation in the dark, the solution was replaced by PBS, and the fluorescence intensities of annexin V-FITC and PI were measured using a FilterMax F5 Multi-Mode Microplate Reader.

## Statistical Analysis

Data values are expressed as mean  $\pm$  standard errors of the means (SEMs) and were statistically evaluated using analysis of variance (ANOVA) followed by Bonferroni multiple comparisons tests.

Differences with  $p$  values of less than 0.05 were considered statistically significant. Data analyses were performed using GraphPad Prism software. All quantitative experiments were conducted with at least two independent experiments and four replicates per experiment.

## Results and Discussion

### Cytotoxicity Assay

Assays to determine the *in vitro* cytotoxicity of resveratrol, colchicine, and hydroxyurea were performed to estimate the optimal concentrations of these compounds for fluorescence tests and MN assays. Positive and negative controls were used to check assay performance and to validate results. Table 1 shows cell viability percentage results in the cytotoxicity assays.

**Table 1:** Cell viability results in the cytotoxicity assay by neutral red uptake method for resveratrol, colchicine, and hydroxyurea.

Extract Concentration (%)	Cell Viability $\pm$ cv (%)				
	Resveratrol	Colchicine	Hydroxyurea	Positive control	Negative control
100	30.76 $\pm$ 13.07	100.81 $\pm$ 9.28	2.44 $\pm$ 0.00	1.13 $\pm$ 0.00	91.60 $\pm$ 6.68
50	80.89 $\pm$ 7.74	92.28 $\pm$ 4.58	38.86 $\pm$ 12.87	2.96 $\pm$ 0.72	98.18 $\pm$ 3.16
25	91.94 $\pm$ 6.01	92.28 $\pm$ 4.06	106.10 $\pm$ 11.00	96.76 $\pm$ 1.40	102.51 $\pm$ 2.67
12.5	99.37 $\pm$ 7.18	94.96 $\pm$ 10.11	111.87 $\pm$ 6.56	94.06 $\pm$ 6.37	104.40 $\pm$ 2.49
6.25	99.52 $\pm$ 7.53	96.18 $\pm$ 13.35	97.64 $\pm$ 9.91	96.67 $\pm$ 7.68	105.19 $\pm$ 3.82

cv: coefficient of variation.

The cytotoxicity index ( $IC_{50}$ ) was estimated by graphical analysis in Figure 1 using the intersection of the  $IC_{50}$  line and the cell viability

curve. In this analysis, the negative control showed no toxicity. The positive control presented an  $IC_{50}$  of about 37 % indicating that at this concentration the positive control caused injury or death to 50 % of the cell population in the assay. Resveratrol showed cytotoxic effect with  $IC_{50}$  of about 80 %, corresponding to a concentration of 401.5  $\mu$ M. Hydroxyurea showed cytotoxicity with an  $IC_{50}$  value of approximately 46 %, corresponding to 11.8 mg/mL Colchicine presented no cytotoxicity, like the negative control, up to the concentration of 128  $\mu$ g/mL.

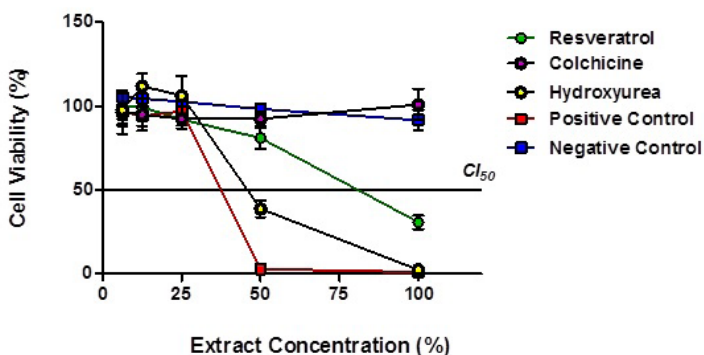


**Figure 1:** Cell viability curves of resveratrol, colchicine, and hydroxyurea in the cytotoxicity assay.

## Analysis of the $LD_{50}$ of Ionizing Radiation

Analyses of lethal doses of ionizing radiation were performed to define the dose of radiation that promoted cell death in 50 % of the cell population in order to verify the combined effects of resveratrol and radiation on NCI-H292 cell culture.

Figure 2 shows the cell survival curve. From these analyses, it was found that the  $LD_{50}$  value was about 693 Gy.

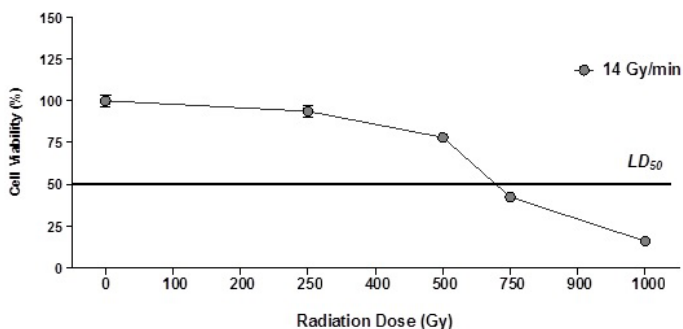


**Figure 2:** Cell survival curve of the ionizing radiation lethal dose assay.

## Micronucleus Assays

The genotoxic effects of resveratrol in cells exposed to ionizing radiation was verified by cytokinesis-block MN technique. MN on binucleated cells (BNCs) was identified by acridine orange staining of NCI-H292 cells culture, as shown in Figure 3.

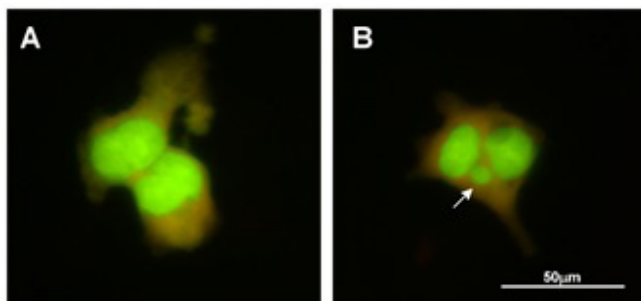


**Figure 3:** Typical aspect of binucleated NCI-H292 cell after acridine orange staining. (A) Binucleated cells. (B) MN in binucleated cell (20× magnification).

Microscopically, the nuclei and MN are observed as bright green staining, and cytoplasm is observed as red staining. In this analysis one MN formation was observed per cell.

Figure 4 shows MN scoring of cultured cells exposed to different resveratrol concentrations and ionizing radiation doses. OECD 487 [19] recommends that at least one mitosis process per cell is observed for the analysis of MN frequencies during exposure of the cells to cytochalasin-B. Our results showed that the interaction between resveratrol and radiation was significant ( $p < 0.01$  and  $p < 0.05$ ). Additionally, resveratrol (15 and 60  $\mu\text{M}$ ) induced a significant increase in the frequency of MN formation in NCI-H292 cell cultures exposed to 5 Gy dose ( $p < 0.01$ ). Resveratrol (30  $\mu\text{M}$ ) also induced a significantly increased frequency of MN formation in nonirradiated and irradiated (0.8 Gy) NCI-H292 cells ( $p < 0.01$  and  $p < 0.05$ ).

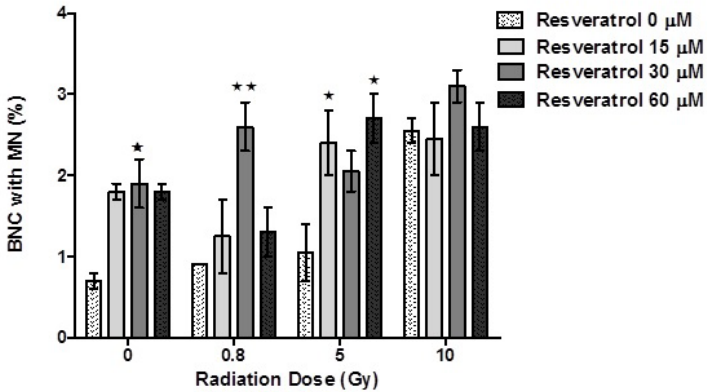


**Figure 4:** MN frequencies in NCI-H292 cells exposed to resveratrol and ionizing radiation. Error bars represent standard errors of the means (SEMs).  $p < 0.05$ ,  $p < 0.01$ .

Figure 5 shows the cytokinesis block proliferation index (CBPI) of cultured cells exposed to different resveratrol concentrations and ionizing radiation doses. The interactions between resveratrol and radiation effects were significant ( $p < 0.05$ ,  $p < 0.01$ ,  $p < 0.001$ ) based on CBPIs. Moreover, the number of cell cycles per cell during exposure to cytochalasin-B differed among groups. NCI-H292 cells exposed to resveratrol (15  $\mu\text{M}$ ) and 5 and 10 Gy doses showed significantly decreased numbers of cell cycles per cell ( $p < 0.05$ ,  $p < 0.01$ ). 30  $\mu\text{M}$

resveratrol in nonirradiated and irradiated NCI-H292 cells at 10 Gy dose also showed significantly decreased numbers of cell cycles per cell ( $p < 0.01$ ,  $p < 0.05$ ). Moreover, in NCI-H292 cells exposed to 10 Gy, 60  $\mu\text{M}$  resveratrol induced a significant decrease in the number of cell cycles per cell during exposure to cytochalasin-B ( $p < 0.001$ ).

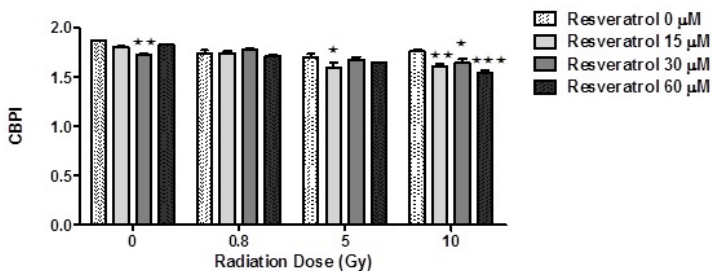


**Figure 5:** CBPI of NCI-H292 cells exposed to resveratrol and ionizing radiation. Error bars represent standard error of the means (SEMs).  $p < 0.05$ ,  $p < 0.01$ ,  $p < 0.001$ .

The genotoxic effects of resveratrol have recently been verified in cultures of Chinese hamster lung fibroblasts and mouse lymphoma cells. In a study by Jeong et al. [20], the genotoxic activity of resveratrol observed was lower when the concentration was minor than 62  $\mu\text{g}/\text{mL}$  (272  $\mu\text{M}$ ). In another study by Fox et al. [21], resveratrol was found to induce severe genotoxic effects without promoting cellular mutagenesis. Moreover, 92  $\mu\text{M}$  resveratrol was shown to have high genotoxic potential in cultures of KB-V1 human carcinoma cells, which are resistant to chemotherapeutics. Consistent with these findings, our results showed that 15, 30, and 60  $\mu\text{M}$  resveratrol increased MN frequencies in NCI-H292 cells exposed to different doses of ionizing radiation.

*In vitro* MN assays have methodological advantages related to reduced cost, increased speed of obtaining reliable results, and reduced use of laboratory animals [22]. Therefore, *in vitro* MN assays are an excellent option for verifying the genotoxic effects of resveratrol in different cell lines.

## Cell Cycle Analyses by Fluorescence Assays

To investigate if resveratrol ( $IC_{50}$ , 401.5  $\mu$ M) induces cell cycle synchronization, NCI-H292 cells were treated with colchicine ( $IC_{50}$ , > 128.0  $\mu$ g/mL) and hydroxyurea ( $IC_{50}$  - 11.8 mg/mL), and they were exposed to different doses of ionizing radiation.

According to the literature, colchicine induces cell cycle synchronization in the mitosis phase (M phase). In contrast, hydroxyurea blocks the cell cycle in the synthesis phase (S phase) [23,24]. The M phase is more sensitive, whereas the S phase is more resistant to the effects of ionizing radiation [2].

Ethidium bromide stains unhealthy cells in its final stages of apoptosis or necrosis, allowing the visualization of injured cells as red-orange staining. Table 2 summarizes ethidium bromide fluorescence intensity values measured 3 h after cells irradiation.

**Table 2:** Ethidium bromide fluorescence intensity values measured 3 h after cells irradiation.

Sample	Fluorescence intensities at different radiation doses			
	0	0.8	5	10
Control	6794 $\pm$ 8	6926 $\pm$ 7	6962 $\pm$ 2	7211 $\pm$ 5
Resveratrol (15 $\mu$ M)	6618 $\pm$ 4	6708 $\pm$ 0	6817 $\pm$ 3	6604 $\pm$ 9
Resveratrol (30 $\mu$ M)	6658 $\pm$ 8	7170 $\pm$ 7	7098 $\pm$ 7	6458 $\pm$ 7
Resveratrol (60 $\mu$ M)	6351 $\pm$ 6	6484 $\pm$ 6	6699 $\pm$ 3	6395 $\pm$ 13
Colchicine (0.08 $\mu$ g/mL)	7041 $\pm$ 9	7144 $\pm$ 1	7184 $\pm$ 11	6344 $\pm$ 8
Hydroxyurea (152.12 $\mu$ g/mL)	6832 $\pm$ 6	7204 $\pm$ 11	7163 $\pm$ 5	7270 $\pm$ 9

Values represent the means  $\pm$  SEMs of three separate experiments ( $n = 3$ ).

As shown in Figure 6, cells stained with ethidium bromide 3 h after radiation were similar for all samples analyzed, without any significant differences.

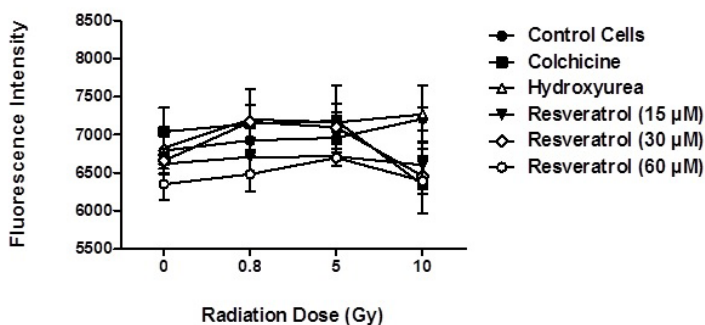


**Figure 6:** Ethidium bromide fluorescence intensity measured 3 h after irradiation at different doses. Points represent the means  $\pm$  SEMs of three separate experiments ( $n = 3$ ).

Table 3 shows ethidium bromide fluorescence intensity values measured 24 h after cells irradiation.

**Table 3:** Ethidium bromide fluorescence intensity values measured 24 h after cells irradiation.

Sample	Fluorescence intensities at different radiation doses			
	0	0.8	5	10
Control	6819 $\pm$ 4	7776 $\pm$ 3	7841 $\pm$ 5	7337 $\pm$ 3
Resveratrol (15 $\mu$ M)	6743 $\pm$ 7	6625 $\pm$ 10	6971 $\pm$ 6	8373 $\pm$ 6
Resveratrol (30 $\mu$ M)	22265 $\pm$ 5	22377 $\pm$ 4	22694 $\pm$ 2	33196 $\pm$ 7
Resveratrol (60 $\mu$ M)	7198 $\pm$ 3	6987 $\pm$ 3	6957 $\pm$ 3	6733 $\pm$ 3
Colchicine (0.08 $\mu$ g/mL)	7315 $\pm$ 4	8300 $\pm$ 16	8363 $\pm$ 11	8123 $\pm$ 0
Hydroxyurea (152.12 $\mu$ g/mL)	7357 $\pm$ 5	7362 $\pm$ 7	7425 $\pm$ 7	3858 $\pm$ 12

Values represent the means  $\pm$  SEMs of three separate experiments ( $n = 3$ ).

As shown in Figure 7, only 30  $\mu\text{M}$  resveratrol induced a significant increase of injured cells when associated with different radiation doses ( $p < 0.001$ ). Moreover, the cell cycle synchronization effect was not observed in any cells exposed to resveratrol, hydroxyurea, or colchicine at 3 and 24 h after cells irradiation.

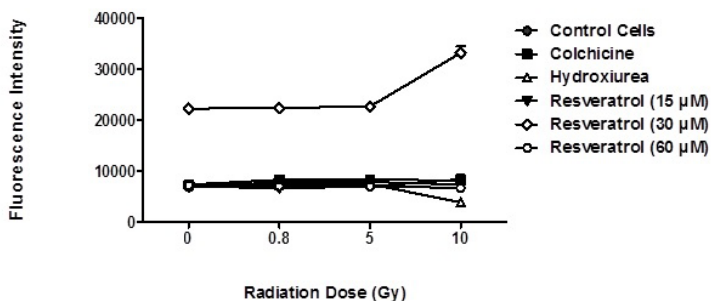


**Figure 7:** Ethidium bromide fluorescence intensity measured 24 h after cells irradiation. Points represent the means  $\pm$  SEMs of three separate experiments ( $n = 3$ ).

## DNA Repair and Cell Injury Analysis by Fluorescence Assays

To investigate DNA repair, the fluorescent intensity of cells was analyzed at 3 and 24 h after cells irradiation. As shown in Figure 8, DNA repair was not observed in any of the analyzed samples. However, cells exposed to 30  $\mu\text{M}$  resveratrol and at different doses of radiation or nonirradiated showed a significant increase of injured cells ( $p < 0.001$ ). Cells exposed to 15  $\mu\text{M}$  resveratrol at 10 Gy ( $p < 0.05$ ) and control cells at 5 Gy ( $p < 0.001$ ) showed a significant increase in injured cells at 24 h after cells irradiation.

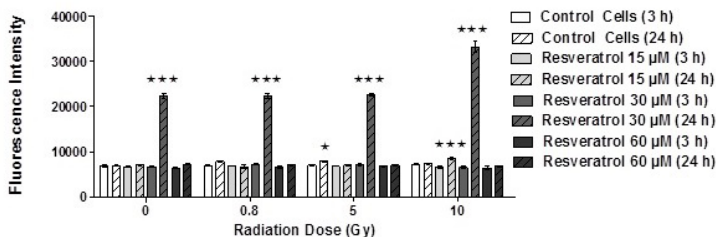


**Figure 8:** Ethidium bromide fluorescence intensity measured 3 h and 24 h after cells irradiation. Each data point represents the means  $\pm$  SEMs of three separate experiments ( $n = 3$ ).  $p < 0.05$ ,  $p < 0.001$ .

Consistent with our findings, a recent study by Magalhães et al. [25] demonstrated that resveratrol (15, 30, and 60  $\mu\text{M}$ ) did not induce cell repair processes in human rhabdomyosarcoma cell cultures at 24 and 48 h after exposure to gamma radiation (50 and 100 Gy).

To understand the increase of injured cells induction of resveratrol, there was conducted an apoptosis and necrosis analysis. It was investigated in the NCI-H292 cells exposed to resveratrol and ionizing radiation.

Tables 4 and 5 present the annexin V-FITC and PI fluorescence intensity values measured 24 h after cells irradiation.

**Table 4:** Annexin V-FITC fluorescence intensity values measured 24 h after cells irradiation.

Sample	Fluorescence intensities at different radiation doses			
	0	0.8	5	10
Control	13010 ± 5	15462 ± 3	14237 ± 6	15036 ± 1
Resveratrol (15 µM)	10891 ± 15	14020 ± 6	15984 ± 9	11905 ± 9
Resveratrol (30 µM)	80131 ± 2	15611 ± 2	18566 ± 6	84828 ± 6
Resveratrol (60 µM)	12765 ± 10	25287 ± 9	27573 ± 9	15963 ± 2
Colchicine (0.08 µg/mL)	14368 ± 11	16331 ± 9	14627 ± 9	21352 ± 10
Hydroxyurea (152.12 µg/mL)	12041 ± 0	14045 ± 6	15107 ± 10	14860 ± 0

Values represent the means ± SEMs of two separate experiments ( $n = 2$ ).

**Table 5:** PI fluorescence intensity values measured 24 h after cells irradiation.

Sample	Fluorescence intensities at different radiation doses			
	0	0.8	5	10
Control	139 ± 6	20 ± 7	204 ± 5	169 ± 5
Resveratrol (15 µM)	143 ± 15	14 ± 0	114 ± 11	119 ± 7
Resveratrol (30 µM)	529 ± 5	20 ± 14	144 ± 18	631 ± 1
Resveratrol (60 µM)	153 ± 4	30 ± 19	104 ± 16	156 ± 1
Colchicine (0.08 µg/mL)	167 ± 13	20 ± 9	159 ± 9	195 ± 11
Hydroxyurea (152.12 µg/mL)	153 ± 18	24 ± 15	100 ± 1	153 ± 8

Values represent the means ± SEMs of two separate experiments ( $n = 2$ ).

Figure 9 shows apoptosis and necrosis detection by annexin V-FITC and PI staining. The results showed that NCI-H292 cells exposed to 30  $\mu\text{M}$  resveratrol nonirradiated and irradiated at 10 Gy dose were stained by both annexin V-FITC and PI, indicating induction of cellular necrosis. The other samples showed negative results for annexin V-FITC and PI analyses, indicating that cells remained viable. Apoptotic cells were measured but not detected in this analysis; hence, apoptotic cells were stained only by annexin V-FITC. Therefore, 30  $\mu\text{M}$  resveratrol showed radiosensitive effects in NCI-H292 cells exposed to ionizing radiation at 10 Gy dose.

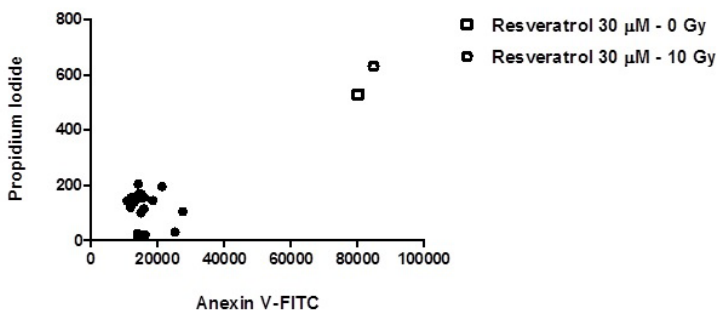


**Figure 9:** Apoptosis and necrosis in NCI-H292 cells detected by annexin V-FITC and PI staining. Each data point represents the means  $\pm$  SEMs of two separate experiments ( $n = 2$ ).

Similar results have indicated that resveratrol induces late apoptotic and necrotic cell death through different mechanisms in many types of cancer cells [26-28]. According Magalhães et al. [25], resveratrol (15  $\mu\text{M}$ ) has potent radioprotective effects in human rhabdomyosarcoma cells exposed to gamma radiation (50 Gy) after 48 h. In addition, Moreno et al. [29] demonstrated that resveratrol (25 and 30  $\mu\text{M}$ ) has radioprotective effects in normal NCTC L929 cells irradiated with gamma rays at doses of 500 and 800 Gy. In lung cancer cells, an

*in vitro* study conducted by Liao et al. [13] showed that resveratrol (25  $\mu\text{M}$ ) induced nuclear fragmentation in human NCI-H838 non-small cell lung cancer cells exposed to radiation at 6 MeV of electron beam energy (2 Gy). Moreover, resveratrol has been shown to have both radiosensitive and radioprotective potential in many types of tumor cells according to the cell type, resveratrol concentration, radiation type, and radiation dose [30,31].

## Conclusion

In this study, was observed that when mucoepidermoid lung carcinoma cells (NCI-H292) are exposed to resveratrol at 30  $\mu\text{M}$  concentration prior to irradiation at 0.8, 5, and 10 Gy doses there was an increase of the injured cells, observed 24h after irradiation. Moreover, 30  $\mu\text{M}$  resveratrol in combination or not with ionizing radiation (10 Gy) induced necrosis in NCI-H292 cells analyzed 24 h after irradiation. Resveratrol at 15, 30, and 60  $\mu\text{M}$  concentrations increased MN frequencies in NCI-H292 cells exposed to different doses of ionizing radiation.

Therefore, resveratrol in combination with radiation showed a great potential to cause DNA damage in NCI-H929 cells. Further studies about the radiosensitive and radioprotective potentials of resveratrol in tumor cells are necessary in order to improve strategies for ionizing radiation cancer treatments. DNA repair and cell cycle synchronization effects were not observed.

## Acknowledgments

The authors would like to thank Rezolina P. Santos from Instituto Adolfo Lutz (São Paulo) for cellular microplate preparation, and Fundação de Amparo à Pesquisa do Estado de São Paulo (FAPESP) by the Research Grant Process Number 2013/03791-9.

## References

1. Torre LA, Bray F, Siegel RL, Ferlay J, Lortet-Tieulent J, et al. Global cancer statistics, 2012. *CA: A Cancer Journal for Clinicians*. 2015; 65: 87-108.
2. Halperin EC, Wazer DE, Perez CA, Brady LW. *Perez & Brady's principles and practice of radiation oncology*. Philadelphia: Lippincott Williams & Wilkins. 2013.
3. Xu HT, Lin XY, Li QC, Wang EH. The alveolar epithelial differentiation of glandular inner lining cells in a mucoepidermoid carcinoma of the lung: a case report. *Diagnostic Pathology*. 2012; 7: 1-5.
4. Huang HK, Cheng YL, Gang H, Tzao C, Lee SC. Mucoepidermoid Carcinoma of the lung. *Journal of Medical Sciences*. 2009; 29: 305-308.
5. Fajardo LE, Berthrong M, Anderson RE. *Radiation Pathology*. Hong Kong & Japan: Oxford University Press. 2001.
6. Roth JA, Cox JD, Hong WK. *Lung cancer*. London: Blackwell Science, Inc. 1998.
7. Pervaiz S. Resveratrol: from grapevines to mammalian biology. *The FASEB Journal*. 2003; 17:1975-1985.
8. Leonard SS, Xia C, Jiang BH, Stinefelt B, Klandorf H, et al. Resveratrol scavenges reactive oxygen species and effects radical-induced cellular response. *Biochemical and Biophysical Research Communications*. 2003; 309:1017-1026.
9. Pervaiz S. Chemotherapeutic potential of the chemopreventive phytoalexin resveratrol. *Drug Resistance Updates*. 2004; 7: 333-344.
10. Zoheri I, Bradbury CM, Curry HA, Bisht KS, Goswami PC, et al. Radiosensitizing and anti-proliferative effects of res-

- veratrol in two human cervical tumor cell lines. *Cancer Letters*. 2002; 175: 165-173.
11. Ahamd N, Adhami VM, Afaq F, Feyes DK, Mukhtar H. Resveratrol causes WAF-1/p21-mediated G (1)-phase arrest of cell cycle and induction of apoptosis in human epidermoid carcinoma A431 cells. *Clinical Cancer Research*. 2001; 7:1466-1473.
  12. Hosseini A, Ghorbani A. Cancer therapy with phytochemicals: evidence from clinical studies. *Avicenna Journal of Phytomedicine*. 2015; 5: 84-97.
  13. Liao HF, Kuo CD, Yang YC, Lin CP, Tai HC, et al. Resveratrol enhances radiosensitivity of human non-small cell lung cancer NCI-H838 cells accompanied by inhibition of nuclear factor-kappa B activation. *Journal of Radiation Research*. 2005; 46: 387-393.
  14. International Organization for Standardization (ISO document 10 993-5). Biological evaluation of medical devices, Part 5, Tests for cytotoxicity: in vitro methods. 2009.
  15. Rogero SO, Lugão AB, Ikeda TI, Cruz AS. Teste *in vitro* de Citotoxicidade: Estudo comparativo entre duas metodologias. *Materials Research*. 2003; 6: 317-329.
  16. Fenech M. The in vitro micronucleus technique. *Mutation Research*. 2000; 455: 81-95.
  17. Fenech M. Cytokinesis-block micronucleus cytome assay. *Nature Protocols*. 2007; 2: 1084-1104.
  18. Heddle JA, Fenech M, Hayashi M, MacGregor JT. Reflections on the development of micronucleus assays. *Mutagenesis*. 2011; 26: 3-10.
  19. Organization for Economic Co-operation and Development (OECD 487). Guideline for the testing of chemicals, Pro-

- posal for updating test guideline 487: in vitro mammalian cell micronucleus test. 2012.
20. Jeong MH, Yang K, Lee CG, Jeong DH, Park YS, et al. In vitro genotoxicity assessment of a novel resveratrol analogue, HS-1793. *Toxicological Research*. 2014; 3: 211-220.
  21. Fox JT, Sakamuru S, Huang R, Teneva N, Simmons SO, et al. High-throughput genotoxicity assay identifies antioxidants as inducers of DNA damage response and cell death. *Proceedings of the National Academy of Sciences of the United States of America*. PNAS. 2012; 109: 5423-5428.
  22. Flores M, Yamaguchi MU. Teste do micronúcleo: uma triagem para avaliação genotóxica. *Revista Saúde e Pesquisa*. 2008; 1: 337-340.
  23. Neill C, Guest W. The effects of hydroxyurea on cultured somatic cells of the chinese hamster, *cricketulus griseus*. *Arkansas Academy of Science Proceedings*. 1967; 21: 59-63.
  24. Blajeski AL; Phan VA, Kottke TJ, Kaufmann SH. G1 and G2 cell-cycle arrest following microtubule depolymerization in human breast cancer cells. *The Journal of Clinical Investigation*. 2002; 110: 91-99.
  25. Magalhães VD, Rogero SO, Cruz AS, Vieira DP, Okazaki K, et al. In vitro tests of resveratrol radiomodifying effect on rhabdomyosarcoma cells by comet assay. *Toxicology in Vitro*. 2014; 28: 1436-1442.
  26. Lang F, Qin Z, Li F, Zhang H, Fang Z, et al. Apoptotic cell death induced by resveratrol is partially mediated by the autophagy pathway in human ovarian cancer cells. *Plos One Journal* *Pone*. 2015; 10: 1-17.
  27. Whyte L, Huang YY, Torres K, Mehta RG. Molecular mechanisms of resveratrol action in lung cancer cells using dual

- protein and microarray analyses. *Cancer Research*. 2007; 67: 12007-12017.
28. Luo H, Wang L, Schulte BA, Yang A, Tang S. Resveratrol enhances ionizing radiation-induced premature senescence in lung cancer cells. *International Journal of Oncology*. 2013; 43: 1999-2006.
  29. Moreno CS, Rogero SO, Ikeda TI, Cruz AS, Rogero JR. Resveratrol and radiation biological effects. *International Journal of Nutrology*. 2012; 5: 28-33.
  30. Heiduschka G, Lill C, Seemann R, Brunner M, Schmid R, et al. The effect of resveratrol in combination with irradiation and chemotherapy: study using Merkel cell carcinoma cell lines. *Strahlentherapie und Onkologie*. 2014; 190: 75-80.
  31. Sebastià N, Almonacid M, Villaescusa JI, Cervera J, Such E, et al. Radioprotective activity and cytogenetic effect of resveratrol in human lymphocytes: An in vitro evaluation. *Food and Chemical Toxicology*. 2013; 51:391-395.